

Interpreting atomic force microscopy measurements of hydrodynamic and surface forces with nonlinear parametric estimation

Song Cui,¹ Rogerio Manica,^{2,a)} Rico F. Tabor,^{3,4} and Derek Y. C. Chan^{2,4,5,b)}

¹*Institute of Materials Research and Engineering, 3 Research Link, Singapore 117602*

²*Institute of High Performance Computing, 1 Fusionopolis Way, Singapore 138632*

³*School of Chemistry, Monash University, Clayton, VIC 3800, Australia*

⁴*Particulate Fluids Processing Centre, The University of Melbourne, Parkville, VIC 3010, Australia*

⁵*Faculty of Life and Social Sciences, Swinburne University of Technology, Hawthorn, VIC 3122, Australia*

(Received 6 August 2012; accepted 16 September 2012; published online 8 October 2012)

A nonlinear parameter estimation method has been developed to extract the separation-dependent surface force and cantilever spring constant from atomic force microscope data taken at different speeds for the interaction between a silica colloidal probe and plate in aqueous solution. The distinguishing feature of this approach is that it exploits information from the velocity dependence of the force-displacement data due to hydrodynamic interaction to provide an unbiased estimate of the functional form of the separation-dependent surface force. An assumed function for the surface force with unknown parameters is not required. In addition, the analysis also yields a consistent estimate of the *in situ* cantilever spring constant. In combination with data from static force measurements, this approach can further be used to quantify the extent of hydrodynamic slip. © 2012 American Institute of Physics. [<http://dx.doi.org/10.1063/1.4756044>]

I. INTRODUCTION

For over 20 years, the atomic force microscope (AFM) has been used successfully for imaging, direct force measurement, and manipulating matter at the nanoscale. It continues to be a valuable research tool to extend our understanding of fundamental processes down to atomic level under ambient conditions. A particularly common application is to use the AFM to measure the force between a colloidal particle attached to the tip of the microcantilever and a substrate in different aqueous environments. The goal is to extract the variation of the force between the particle and the substrate with separation. The general operations of the AFM¹ and specific application for dynamic force measurements between soft materials² has also been reviewed recently. Accurate force measurements depend critically on the precise knowledge of the effective spring constant of the force-sensing microcantilever, an integral component of the AFM. Due to inherent fabrication tolerances,³ determination of the *in situ* cantilever spring constant that includes the effect of the attached particle is highly desirable.¹

The current generation of AFM has the capacity to acquire force data at high sampling rates and at different drive speeds or scan rates. It is therefore timely to exploit such advances in data density and develop new ways to extract information about the force as a function of the separation between the interacting surfaces.

In the traditional analysis of equilibrium force measurements, it is common to assume a functional form for the force-separation relation that contains one or more parameters to be fitted to experimental data. In such endeavours, it is important to have an accurate estimate of the separation. Due to the

small size of the interaction zone in the AFM it is difficult to ascertain accurately the absolute separation. Indeed, if adhesive contact does not occur, such as when the interaction is always repulsive, the regime of constant compliance that corresponds to zero separation cannot be determined without ambiguity. One attempt to address this issue is to exploit changes in the scattering of evanescent light waves when surfaces are in close proximity to provide a point of reference for “zero separation”.⁴ Alternatively, laser-scanning confocal microscopy has been employed to measure an accurate initial separation to calibrate dynamic AFM force measurements between colloidal bodies.⁵ However, it is not always practical or feasible to implement such additional measurements. And when it comes to investigating new types of interactions for which the theory is less well developed, a suitable functional form may not be readily available.

The AFM is also used to investigate hydrodynamic slip during fluid flow between surfaces at nanoscale separations. Results indicate that the degree of slip appears to depend on the type of cantilever that is being used.^{6,7} More recent AFM studies of hydrodynamic slip with fluids with viscosities about 50 times that of water and driven at speeds of up to 80 $\mu\text{m/s}$ require non-Newtonian fluid models that include shear-rate dependent viscosities and additional fitting parameters.⁸

Against this background we have developed a nonlinear parametric estimation approach that takes force data measured at different velocities to extract the force-separation relationship and the *in situ* spring constant in an unbiased fashion. In particular, this method of data analysis does not require an *a priori* functional form of the force-separation formula containing parameters to be fitted. The robustness and sensitivity of this approach have been tested using synthetic data. The method is then applied to experimental force-separation data that have been acquired at higher densities

^{a)}E-mail: manicar@ihpc.a-star.edu.sg.

^{b)}E-mail: d.chan@unimelb.edu.au.

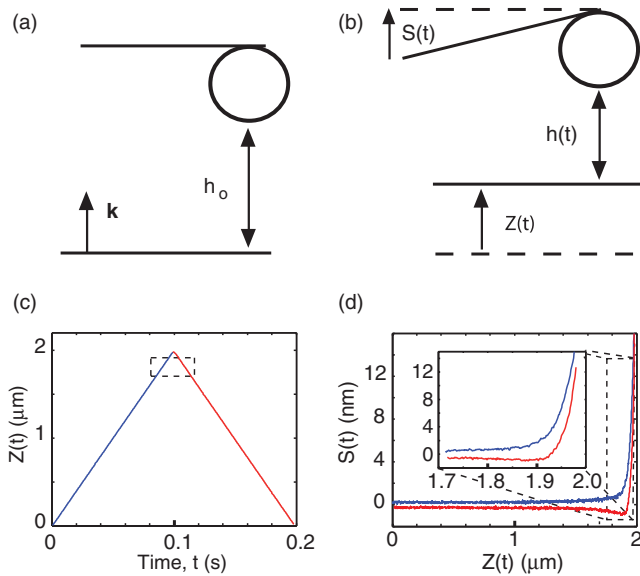


FIG. 1. A schematic of the AFM showing the colloid probe on the cantilever (a) at the initial configuration and (b) at separation, $h(t)$ between the colloid and substrate with cantilever deflection, $S(t)$. (c) The displacement function, $Z(t)$ at nominal velocity $20 \mu\text{m/s}$ and (d) experimental $S(t)$ vs $Z(t)$ data for a silica particle (radius $10 \mu\text{m}$) against a silica plate in 0.27 mM univalent aqueous electrolyte. Data within the dashed rectangle are used in our parametric estimation.

than normal. Our investigation led us to suggest modifications to force measurement protocols that can potentially improve the usability of data from such AFM measurements. Given the central importance of aqueous solutions in many technological and biological applications, we can assume a Newtonian liquid and that the magnitude of surface forces and hydrodynamic forces at the typical drive speeds are comparable.

To preface the development of our parametric estimation method, we first recapitulate in Sec. II the key elements of using an AFM to measure the time-dependent force between a colloidal sphere of radius R and a flat substrate as depicted in Fig. 1. Then we demonstrate how to construct a cost function or a residual function from experimental data that is to be minimized to extract the force-separation curve, the *in situ* cantilever spring constant that includes the effect of the attached particle and the initial separation between the particle and the substrate. The cost function is a measure of the residual deviation between a theoretically generated set of points and the corresponding experimentally measured set. In Sec. III, we give an example of the cost function or residual function constructed from dynamic force data and provide results obtained from the optimization method. In Sec. IV, we discuss variations of the results due to different physical assumptions, namely, the possible hydrodynamic slip at the surfaces of the particle and the substrate and suggest a resolution using results from both static and dynamic force measurements. The main findings are summarized in the Conclusion.

II. THEORETICAL MODEL

Consider the schematic setup to use the AFM to measure forces between a particle and the substrate. The configuration at time $t = 0$ (Fig. 1(a)) is characterized by the unknown initial

separation, h_o , between the colloidal particle (attached to the cantilever) and the substrate. At times $t > 0$, the distance between the particle and the substrate is progressively reduced using a piezo actuator to move the substrate by a measured distance $Z(t) > 0$ (Fig. 1(b)). Repulsion between the particle and the substrate will give rise to a positive cantilever deflection, $S(t) > 0$ that is measured by an optical lever. The common displacement function, $Z(t)$ is an approximate triangular wave, characterized by a nominal velocity that can be adjusted (Fig. 1(c)). Typically, the maximum displacement of $Z(t)$ is about $2 \mu\text{m}$ and sample experimental data for the cantilever deflection $S(t)$ plotted as a function of the displacement $Z(t)$ are given in Fig. 1(d). As a result of hydrodynamic interactions, the deflection data $S(t)$ has an *approach* branch corresponding to *increasing* $Z(t)$ and a *retract* branch corresponding to *decreasing* $Z(t)$. The region in which there are significant differences between these two branches is emphasized in the magnified inset in Fig. 1(d). Our nonlinear parameter estimation method exploits this difference between the approach and retract branch of the $S(t)$ vs $Z(t)$ data which is determined by the relative contribution of hydrodynamic interaction and surface forces.

By balancing forces exerted on the particle due to:

1. the cantilever: $\mathbf{F}_{can} = -K S(t) \mathbf{k}$, with spring constant K ,
2. the interaction with the substrate: $\mathbf{F}_{sur} = 2\pi R E(h(t)) \mathbf{k}$, due to surface force that depends on the instantaneous separation between the particle and the substrate, $h(t)$, and
3. the hydrodynamic interaction: $\mathbf{F}_{hyd} = -[6\pi\mu R^2/h(t)] f_b(h(t))(dh/dt) \mathbf{k}$, arising from relative motion between the particle and the substrate.

we have a relation between the displacement $Z(t)$ and the separation $h(t)$

$$-\frac{6\pi\mu R^2 f_b}{h} \frac{dh}{dt} + 2\pi R E(h) = K S(t) = K [Z(t) + (h(t) - h_o)]. \quad (1)$$

The geometric condition $S = Z + (h - h_o)$ is used in Eq. (1) to relate $(h - h_o)$ to the known quantities: S and Z (Fig. 1(b)). The expression for \mathbf{F}_{hyd} assumes Stokes flow with a provision for the possibility of Navier slip, characterized by a slip length b , at the surface of the particle and of the substrate, via the function:⁹

$$f_b(h) = 2\eta[(1 + \eta) \ln((\eta + 1)/\eta) - 1], \quad (2)$$

with $\eta \equiv hl/(6b)$. The usual no-slip condition corresponds to $b = 0$ when $f_b(h) = 1$. The expression for \mathbf{F}_{sur} assumes the Derjaguin approximation in which $E(h)$ is the interaction energy per unit area between planar surfaces.¹⁰ This is a standard model used for describing AFM experiments that allows hydrodynamic slip.¹¹ However, it is important to note that the present formulation does not require a prescribed or assumed function for $E(h)$. The form of $E(h)$ will instead be determined as an output of our nonlinear parametric estimation method.

The foundation of the parametric estimation method is drawn from control theory. Given a set of experimental data, the method involves constructing a cost function or a residual

function that when minimized with respect to chosen parameter(s) in Eq. (1), will allow us to deduce the form of $E(h)$ as numerical output. Here we choose the initial separation h_o as the parameter, and the output will be the *in situ* spring constant K and the interaction energy per unit area between planar surfaces $E(h)$.

To construct the cost function, we choose a value of h_o and note that the experimental data at discrete time points can be represented as three lists of *approach* data: S_i^a , Z_i^a , and $\Delta h_i^a \equiv h_i^a - h_o \equiv S_i^a - Z_i^a$ with subscript i denoting time at t_i and three lists of *retract* data: S_k^r , Z_k^r and $\Delta h_k^r \equiv h_k^r - h_o \equiv S_k^r - Z_k^r$ at time t_k . We then identify elements in the two vectors Δh^a and Δh^r that have the same value: $\Delta h_\alpha^a = \Delta h_\rho^r$; or equivalently where $S_\alpha^a - Z_\alpha^a = S_\rho^r - Z_\rho^r$ and note the indices α and ρ . In practice, we work with experimental data sets with sufficiently high density so that we can identify the pairs of Δh^a and Δh^r that are within experimental noise (~ 0.1 nm). Using interpolation to improve the match between Δh^a and Δh^r does not make a significant difference.

Suppose we have an estimate of the initial separation, h_o , and we know the value of the slip length, b , then by subtracting the ρ th element of the retract version from the α th element of the approach version of Eq. (1) we obtain

$$H_j(h_o) \equiv \frac{6\pi\mu R^2 f_b(h)}{h} \left(\frac{dh_\alpha^a}{dt} - \frac{dh_\rho^r}{dt} \right) \doteq K (S_\alpha^a - S_\rho^r) \equiv G_j(h_o). \quad (3)$$

The terms $2\pi R E(h)$ from each equation cancel because $\Delta h_\alpha^a + h_o \equiv h \equiv \Delta h_\rho^r + h_o$ by construction and the derivatives dh/dt are calculated numerically. In Eq. (3), the notation \doteq indicates that if the estimated value of h_o is correct, Eq. (1) will be an accurate representation of the experimental data and hence the corresponding elements of the two lists or vectors $\mathbf{G}(h_o)$ and $\mathbf{H}(h_o)$ are equal. Therefore, the objective is to find the value of h_o that will achieve this equality. We do so by constructing a suitable function of $\mathbf{G}(h_o)$ and $\mathbf{H}(h_o)$ from which we can find the correct value of h_o .

First we recall the Schwarz inequality: $\|\mathbf{G} \cdot \mathbf{G}\| \|\mathbf{H} \cdot \mathbf{H}\| \geq \|\mathbf{G} \cdot \mathbf{H}\|^2$ that is obeyed by any two vectors, and the equality holds when the two vectors are equal (or when one or both vectors are zero, which does not apply in the present context). We construct a positive definite cost function or residual function based on this inequality

$$C(h_o) \equiv \sum_i G_i^2 - \frac{\sum_i (G_i H_i)^2}{\sum_i H_i^2} \geq 0 \quad (4)$$

with the property that if $C(h_o) = 0$ at the particular h_o , then the two vectors $\mathbf{G}(h_o)$ and $\mathbf{H}(h_o)$ will be equal and hence that h_o will be the correct value for which Eq. (1) provides an accurate and ideal representation of the experimental data. In practice, because of experimental noise, the cost function $C(h_o)$ has a single minimum at $h_o = \hat{h}_o$ that represents the best estimate of the correct value of the initial separation based on available noisy experimental data.

The implementation of the nonlinear parametric estimation method therefore involves constructing $C(h_o)$ and then locating numerically the minimum \hat{h}_o . The *in situ* spring constant of the cantilever with the colloidal probe particle at-

tached is then given by

$$K = \frac{\sum_i H_i^2}{\sum_i G_i H_i} \quad \text{at } h_o = \hat{h}_o \quad (5)$$

and the variation of the interaction energy per unit area with separation is given by evaluating

$$E(h) = \frac{1}{2\pi R} \left[\frac{6\pi\mu R^2}{h} \frac{dh}{dt} + K S \right] \quad \text{at } h_o = \hat{h}_o. \quad (6)$$

The form of $E(h)$ extracted from the approach branch and the retract branch data should agree if the model given by Eq. (1) is correct. This provides a consistency check on this method. Since the model in Eq. (1) allows for the possibility of a Navier slip length b , the estimate of spring constant K , initial separation h_o , and the interaction energy per unit area $E(h)$ will depend on the assumed value of b .

III. SAMPLE COST FUNCTION

The general shape of the cost function $C(h_o)$ is shown in Fig. 2. It has one sharp minimum and the precision in which this can be located – to within ± 1 nm as illustrated in the inset – is required to obtain the desired precision in $E(h)$. The magnitude of $C(h_o)$ at the minimum is controlled by noise in the experimental data and so this value does not contain usable information. Hence we present $C(h_o)$ in arbitrary units.

As an illustration of the parametric estimation method, we measured the interaction between a silica colloidal probe (radius, $R = 10 \mu\text{m}$) and a silica plate in aqueous electrolyte (0.27 mM NaNO_3 , $\text{pH} = 10$). We use the standard triangular waveform as the drive function on the AFM (Asylum Research MFP-3D driven by ARC1 controller) with nominal drive velocities or scan rates of $V = 10, 20, 30$, and $40 \mu\text{m/s}$. The cantilever used was a commercial silicon nitride triangular probe (MLCT, Brüker), to which a borosilicate glass bead had been affixed using two-part epoxy. We set the AFM data acquisition rate to ensure at least 100 force values are

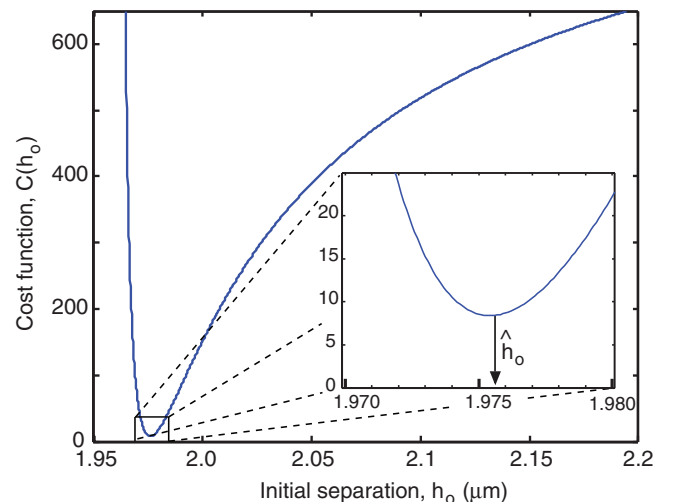


FIG. 2. (a) The cost function $C(h_o)$ with $b = 0$ derived from experimental data at drive velocity, $V = 20 \mu\text{m/s}$ (see text for details). Inset: The precision at which the minimum \hat{h}_o value can be located.

available for constructing the cost function to minimize the effects of experimental noise.

For the experimental system we chose, the particle-plate interaction is expected to be dominated by electrical double layer repulsion for which the interaction energy per unit area can be represented as

$$E_{EDL}(h) = (64nkT/\kappa) \tanh^2(y_o/4) e^{-\kappa h}, \quad (7)$$

where k is the Boltzmann constant, T the temperature, n the number concentration of 1:1 electrolyte with Debye length $1/\kappa$, and $y_o = e\psi_o/kT$ is the scaled surface potential on the silica particle and plate. The expression in Eq. (7) is valid in the superposition regime that we anticipate to hold under our experimental conditions. Literature values of the surface potential of silica under present solution conditions vary between -20 mV and -110 mV.¹² Equation (7) is not used to analyse the experimental data. The form of $E(h)$ is extracted from experimental data using Eq. (6), whereas $E_{EDL}(h)$ in Eq. (7) is used as a convenient way to characterise $E(h)$, assuming it provides reasonable agreement with $E(h)$, in terms of the surface potential ψ_o .

IV. RESULTS

As mentioned earlier, the experimental data needed to construct the cost function in our parametric estimation method should come from the region where the approach and retract branches are sufficiently different. Thus only data in the region delineated in Figs. 1(c) and 1(d) are used for our analysis.

By way of comparison we have also measured very low speed, equilibrium force-displacement data and analyzed the results to extract the force-separation relation by using standard method based on the constant compliance regime to determine the reference for zero separation.

We first take the slip length $b = 0$ and construct cost functions for different drive velocities. Results from the parametric estimation are summarized in Table I. The main features that we observe are:

(i) The deduced value of the spring constant K does not vary systematically with the drive velocity, but is within the range of the uncertainty of the experimental value $K = 0.36 \pm 0.02$ N/m determined by the Hutter method.¹³ The variation can be attributed to noise in the AFM data;

(ii) the deduced form of the interaction energy per unit area $E(h)$ is reassuringly insensitive to the velocity at which the data were acquired (Fig. 3). The separation dependence follows the exponential form given in Eq. (7) with a surface potential, $\psi_o = -47 \pm 3$ mV and the decay length, $1/\kappa = 19 \pm 1$ nm, consistent with the experimental electrolyte concentration of 0.27 mM NaNO₃,

(iii) the interaction energy $E(h)$ deduced by the usual constant compliance analysis of equilibrium data ($V = 0$ in Table I) gives a surface potential, $\psi_o = -50$ mV and Debye length $1/\kappa = 18.0$ nm in Eq. (7), in good agreement with results deduced from dynamic measurements, and

(iv) there is good agreement between the measured force as a function of time and that which is calculated using

TABLE I. Values of the cantilever spring constant, K , and the initial separation, \hat{h}_o , deduced by the parametric estimation method using force data at the indicated drive velocities, V , assuming Navier slip lengths $b = 0$ or 10 nm. The decay length, κ^{-1} and surface potential, ψ_o found by using Eq. (7) to represent the extracted results for $E(h)$ between 10 and 80 nm. The results corresponding to $V = 0$ are obtained from a very low speed measurement and analyzed by reference to the constant compliance regime to estimate the separation.

V ($\mu\text{m/s}$)	b (nm)	K (N/m) (± 0.02)	\hat{h}_o (μm) (± 0.001)	κ^{-1} (nm) (± 1)	ψ_o (mV) (± 2)
0	...	0.36	...	18	-50
10	0	0.37	1.985	19	-45
	10	0.31	1.976	19	-32
20	0	0.37	1.976	19	-47
	10	0.33	1.965	20	-33
30	0	0.36	1.967	19	-47
	10	0.31	1.958	19	-32
40	0	0.35	1.967	20	-50
	10	0.31	1.957	19	-35

Eqs. (1) and (7) with the average values of ψ_o and κ^{-1} and values of h_o taken from Table I (Fig. 4).

By taking the slip length, $b = 0$, the parameter estimation analysis of force data taken at nominal driving velocities between 10 to 40 $\mu\text{m/s}$ gave results for the interaction energy per unit area, $E(h)$ that are consistent with that obtained from constant compliance of equilibrium data. However, if we repeat the parameter estimation method with a slip length $b = 10$ nm we would obtain slightly smaller estimates for the cantilever spring constant, K and a reduction of the initial separation, \hat{h}_o by an amount comparable to b (see Table I). The deduced form of the interaction energy per unit area, $E(h)$ still has the exponential form with an unchanged decay length. However, the change in the estimated initial separation, \hat{h}_o has

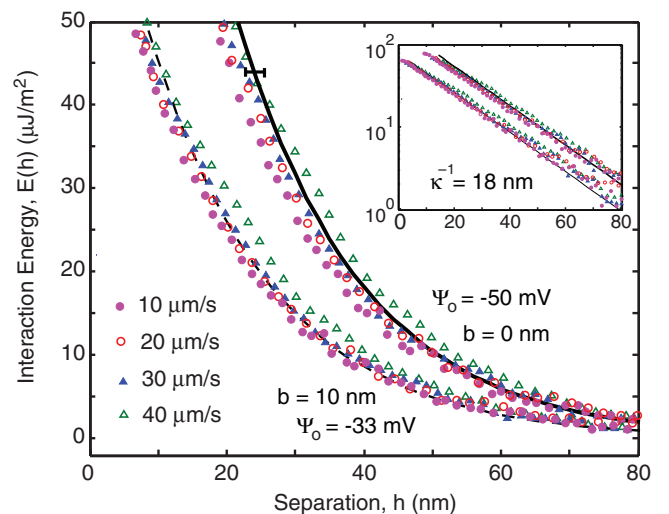


FIG. 3. The interaction free energy per unit area, $E(h)$ obtained by parametric estimation from experimental data at different nominal velocities for an assumed slip length $b = 0$ or 10 nm are shown as symbols. The solid line with indicated error bar is $E(h)$ extracted from constant compliance analysis of equilibrium force data corresponding to a surface potential of -50 mV. The dashed line represent $E(h)$ according to Eq. (7) for the indicated surface potentials and slip lengths. Inset: $E(h)$ plotted on a semi-logarithmic scale.

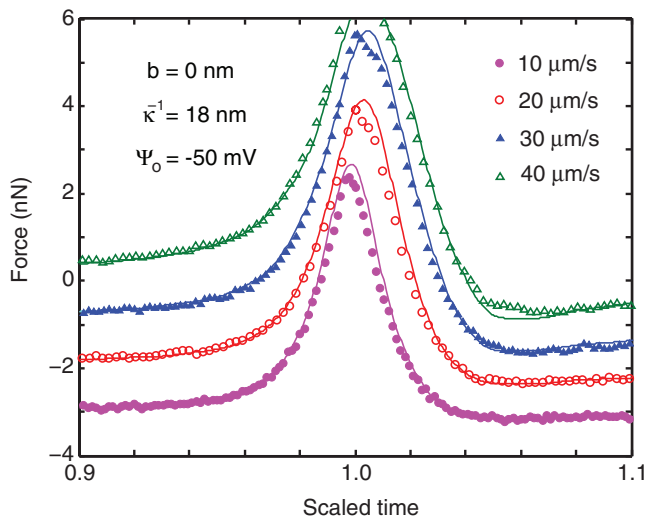


FIG. 4. A comparison of the time variations of the force at drive speeds $V = 10, 20, 30,$ and $40 \mu\text{m/s}$. Symbols: experimental values, lines: from parametric estimation using Eqs. (1) and (7) for $E(h)$ with the indicated parameters and initial separations, h_0 from Table I. Time is scaled by the moment when the AFM piezo drive changes from approach to retract.

the effect of lowering the magnitude of the surface potential to -33 mV , which is at the lower end of the literature range of the silica-electrolyte surface potential. Thus we see by allowing for a non-zero slip length, the force data can still be fitted with an interaction energy per unit area, $E(h)$ that corresponds to a lower surface potential. Therefore we conclude that in using AFM measurement to study the effects of hydrodynamic slip, it would be prudent to check against equilibrium force-displacement data before concluding that there is evidence of slip.

In experiments, we have acquired data points at a higher density than the default value of the AFM software in order to minimize the effects of experimental noise. The signal-to-noise ratio can also be improved by using a different form of the drive function $Z(t)$. The commonly used triangular wave form introduces high amplitude noise from the piezo actuator around the point of maximum travel, so such points cannot be included in the data set for parameter estimation. The use of a smooth waveform may also provide additional low-noise data values for this application.

V. CONCLUSIONS

We have demonstrated that a nonlinear parametric estimation method can be used to analyze dynamic force measurements using the AFM to provide an unbiased estimate of the force-separation relationship between a colloidal particle and a substrate in aqueous environment. This approach also extracts the *in situ* cantilever spring constant and the initial separation.

The accuracy of this method requires a higher data acquisition rate than the default setting on most AFMs to limit the effect of noise on the cost function. The use of smooth piezo actuator displacement functions, and using the closed loop configuration, is also recommended to minimize noise.

When used together with constant compliance analysis of equilibrium force measurements, this approach will be able to resolve the existence or otherwise of hydrodynamic slip at surfaces.

ACKNOWLEDGMENTS

This work has been supported in part by an Australian Research Council Discovery Project Grant to DYCC who is an adjunct professor at the National University of Singapore and a visiting scientist at the Institute of High Performance Computing.

- ¹S. P. McBride and B. M. Law, *Rev. Sci. Instrum.* **81**, 113703 (2010).
- ²R. F. Tabor, F. Grieser, R. R. Dagastine, and D. Y. C. Chan, *J. Colloid Interface Sci.* **371**, 1 (2012).
- ³G. B. Webber, G. W. Stevens, F. Grieser, R. R. Dagastine, and D. Y. C. Chan, *Nanotechnology* **19**, 105709 (2008).
- ⁴C. D. F. Honig and W. A. Ducker, *Phys. Rev. Lett.* **98**, 028305 (2007).
- ⁵R. F. Tabor, H. Lockie, D. Mair, R. Manica, D. Y. C. Chan, F. Grieser, and R. R. Dagastine, *J. Phys. Chem. Lett.* **2**, 961 (2011).
- ⁶T. S. Rodrigues, H.-J. Butt, and E. Bonaccorso, *Colloid Surf., A* **354**, 72 (2010).
- ⁷C. L. Henry and V. S. J. Craig, *Phys. Chem. Chem. Phys.* **11**, 9514 (2009).
- ⁸L. Zhu, P. Attard, and C. Neto, *Langmuir* **28**, 7768 (2012).
- ⁹O. Vinogradova, *Langmuir* **11**, 2213 (1995).
- ¹⁰R. J. Hunter, *Foundations of Colloid Science* (Oxford University Press, 1987), Chap. VII.
- ¹¹C. Neto, D. R. Evans, E. Bonaccorso, H.-J. Butt, and V. S. J. Craig, *Rep. Prog. Phys.* **68**, 2859 (2005).
- ¹²A. P. Legrand, *The Surface Properties of Silicas* (Wiley, Chichester, 1998); L. T. Zhuravlev, *Colloids Surf. A* **173**, 1 (2000).
- ¹³J. L. Hutter and J. Bechhoefer, *Rev. Sci. Instrum.* **64**, 1868 (1993).